

Available at www.sciencedirect.comjournal homepage: www.elsevier.com/locate/he

Rapid charging characterization of $\text{MmNi}_{3.03}\text{Si}_{0.85}\text{Co}_{0.60}\text{Mn}_{0.31}\text{Al}_{0.08}$ alloy used as anodes in Ni–MH batteries

M. Raju^a, M.V. Ananth^a, L. Vijayaraghavan^{b,*}

^aNickel–Metal Hydride Battery Section, Electrochemical Power Systems Division, Central Electrochemical Research Institute, Karaikudi – 630006, India

^bManufacturing Engineering Section, Department of Mechanical Engineering, Indian Institute of Technology Madras, Chennai – 600 036, India

ARTICLE INFO

Article history:

Received 27 December 2008

Received in revised form

5 February 2009

Accepted 9 February 2009

Available online 17 March 2009

Keywords:

Nickel–metal hydride battery

Charge acceptance

Fast charge: hydrogen evolution

Phase transformation

ABSTRACT

The use of Nickel–Metal Hydride (Ni–MH) batteries for traction application in electric and hybrid vehicles is on the rise. High-rate charge/discharge characteristics are important parameters for electric vehicle applications. The ability to reduce charging time is essential in these traction applications. In this paper, the performance of assembled Ni–MH batteries (1.2 V, 0.5 Ah specimen cells) when subjected to different charging rates is described. Changes in battery voltage during charging were monitored with a particular emphasis on the quest for fast recharge characteristics. The charging curves reveal the formation of different types of phases. Hydrogen evolution resulted in flat charge profile after certain amount of overcharging. The changes in discharge level after different rates of charging are insignificant. This paper describes the fast rechargeability of assembled Ni–MH cells under various fast-charge regimes.

© 2009 International Association for Hydrogen Energy. Published by Elsevier Ltd. All rights reserved.

1. Introduction

There is significant interest in energy efficiency and in reducing the dependency on fossil fuels. Increasing efforts are taking place in the introduction of modern electric vehicle and hybrid electric vehicles. Batteries form the heart of electric vehicles. Ni–MH batteries are a viable option for these applications, as they exhibit high specific energy, high specific power and a long cycle life. Besides the energy, power handling, and economy, high tolerance to abuse is an important aspect of the Ni–MH technology. Moreover, they are relatively benign to the environment [1,2]. Reduction in charging duration could make Ni–MH batteries more acceptable for electric vehicle applications.

The possibility of rapid charging a commercial Ni–MH traction battery system at high-rates has already been demonstrated [3]. Although attractive, the Ni–MH system still needs to be proved that it can accept rapid recharge [4]. To facilitate an easy and reliable charging control and to avoid battery premature failure or ageing, it is very important to know the behavior of the battery under a range of charging conditions [1]. Rapid recharge can greatly improve the electric vehicle's mobility and usability and allow the vehicle operator to fully utilize the battery capacity without exceeding the range limit. For hybrid applications, the ability of high power recharge can simplify power control algorithms and improve efficiency to capture regenerative braking power. Fast rechargeability can also facilitate the vehicle operation. The

* Corresponding author. Manufacturing Engineering Section, Department of Mechanical Engineering, Indian Institute of Technology Madras, Chennai – 600036, India. Tel.: +91 44 22574687; fax: +91 44 22570509.

E-mail address: lvijay@iitm.ac.in (L. Vijayaraghavan).

0360-3199/\$ – see front matter © 2009 International Association for Hydrogen Energy. Published by Elsevier Ltd. All rights reserved.

doi:10.1016/j.ijhydene.2009.02.027

battery for electric vehicles generally requires large specific power. The specific power of an advanced battery increases with the high-rate discharge capability of the battery electrode [5–7].

Most Ni–MH batteries are not recommended for fast charge [8] due to the concern of significant heat generation of the system. However, so far limited work has been reported on fast charge of Ni–MH batteries or modules, especially for the electric vehicle applications. Knowledge of the fast-charge control of the Ni–MH batteries (especially, the traction batteries) and their operating limits and underlying mechanisms is therefore crucial to proper utilization and operation of such devices.

Fast charging may also have negative consequences to the battery. For example, fast charging may induce earlier oxygen evolution. This could lead to higher rate of recombinant reaction and reduce charging efficiency. If the oxygen recombination rate is slower than that of oxygen evolution the internal pressure will increase. If the battery response to high charge rates is not properly understood, and adequately monitored and controlled, the battery may be overcharged. Overcharging would lead to considerable temperature increase, excessive gas production, eventual separator degradation, electrolyte loss, and premature failure [9]. The performance of Ni–MH batteries differs in terms of charge and discharge behavior, high-rate discharge capabilities, self-discharge losses, charging efficiency and cycle life [10].

In this work, the performance of Ni–MH batteries assembled by us is discussed. Non-stoichiometric $\text{MmNi}_{3.03}\text{Si}_{0.85}\text{Co}_{0.60}\text{Mn}_{0.31}\text{Al}_{0.08}$ alloy with La/Ce ratio in Mm around 12 was chosen as negative electrode material. This material was identified as the best performing material from the studies on the influence of La/Ce ratio in rare earth based AB_5 -type hydrogen storage alloy used as negative electrodes in Ni–MH batteries [11]. A comparative analysis of the performance observed under different charging rates is presented. The focus of the study is to understand the behavior of battery voltage, charge time, amount of charge input, charge acceptance, and energy efficiency as a function of charging rate. The discharge performance and associated phase transformation during charging is discussed in the present communication.

2. Experimental

Non-stoichiometric lanthanum-rich AB_5 -type rare earth metal-based hydride alloy powder ($\text{MmNi}_{3.03}\text{Si}_{0.85}\text{Co}_{0.60}\text{Mn}_{0.31}\text{Al}_{0.08}$) was used to prepare the negative electrode of the Ni–MH cell. The La/Ce ratio in Mm was 11.65. The purity of the constituent metals (La, Ce, Ni) was at least 99.9%. In order to ensure homogeneity, ingots were turned over and melted twice. The ingots were mechanically pulverized into fine powders of sieve size less than $75\ \mu\text{m}$. The composition of the product was determined by X-ray fluorescence spectroscopy (Horiba XRF analyzer, model XGT-2700).

Test electrodes for galvanostatic charge/discharge experiments were made from 8 g of the alloy and had a geometrical area of $4.5\ \text{cm} \times 9.0\ \text{cm}$. Slurry of the alloy powder with 10% conducting material (carbon powder) and 5% binder (polytetrafluoroethylene) was prepared and subsequently applied

to both sides of a nickel foam substrate. It was compacted and heat-treated at 408 K. The test cell consisted of a three-electrode system in which the metal hydride alloy electrode acted as the working electrode, a sintered $\text{Ni}(\text{OH})_2$ electrode (of higher capacity than the working electrode) as the counter electrode, and an Hg/HgO in 6 M KOH as the reference electrode. Galvanostatic charge/discharge cycling was carried out at a current density of $60\ \text{mA g}^{-1}$ on a Bitrode LCN cycle life tester. Charging was done for 7 h and discharging was done until the potential of the alloy electrode reached $-0.7\ \text{V}$ with respect to the reference electrode. All batteries were subjected to the same test condition. The behavior of the cells is quite consistent through the tests.

The cells were subjected to repetitive charge–discharge cycles so that their performance under different charging regimes could be studied. The temperature was kept at $27\ ^\circ\text{C}$ in the environmental chamber. Battery performance was reproducible, thus 10 cycles were enough to represent the battery behavior under each specific condition. After activation of the electrodes, the cells were undergone at various charge/discharge rates i.e. C/5, C/3, 1C, 2C, 3C and 4C. The synthesis of alloy and electrode preparation procedure is explained elsewhere [12].

3. Results and discussion

The results of overcharging performed at different charging rate (C/5, C/3, 1C, 2C, 3C and 4C) as a function of potential are presented in Fig. 1. It can be seen that the potential profile increases suddenly up to the charging level of $50\ \text{mAhg}^{-1}$ and thereafter exhibits a sloping region with increase in potential. The sloping region comes to a halt at a particular charging level ($\sim 240\ \text{mAhg}^{-1}$) in the case of C/5 and C/3 charging rate and after that, the charging process proceeds without increase in potential. It indicates the evolution of hydrogen. For other charging rates (1C, 2C, 3C and 4C), the charging potential reaches to a peak then gradually decrease as the charging

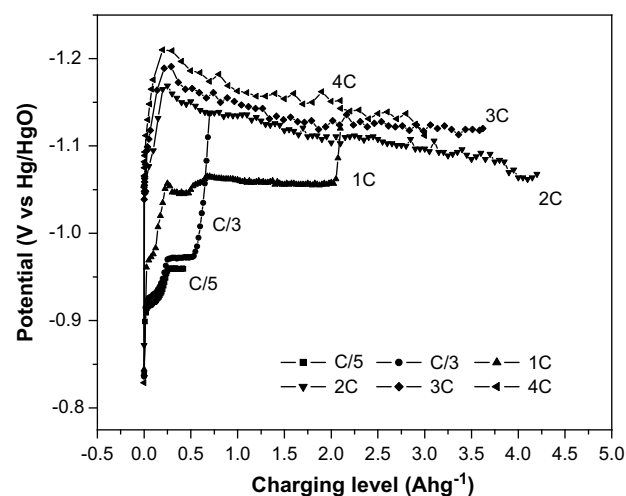


Fig. 1 – Overcharging behavior of $\text{MmNi}_{3.03}\text{Si}_{0.85}\text{Co}_{0.60}\text{Mn}_{0.31}\text{Al}_{0.08}$ alloy metal hydride electrode.

continues. This behavior indicates the hydrogen evolution and heat generation during charging [8]. As a matter of fact, it has been reported that charging even under mild conditions such as 0.1C rate, the Ni–MH battery reveals a temperature increase of more than 9 °C [1]. The battery temperature increases obviously when charged at higher rates and overcharge can result in an increasingly higher temperature rise with steep temperature gradient [13].

Hydrogen absorption reaches a saturation value at the peak potential. Any further charging leads to liberation of hydrogen at the negative electrode. The liberated hydrogen may take part in a recombination reaction with the oxygen liberated at the positive electrode. Since the oxygen recombinant reaction does not consume all the hydrogen evolved at the negative electrode [14], charging the battery at low rates might create adverse effects on battery life due to the loss of hydrogen to the ambient environment and rapid charging is beneficial. In addition, the rollover of the cell voltage is typically observed in oxygen recombinant reaction.

The charging curves are indicative of phase changes occurring during hydrogen absorption. The charge curve at C/3 rate (Fig. 2) clearly depicts this transformation. The charging curve could be divided into different regions and each region represents the particular phase field. As illustrated by Nakamura et al. [15], the region AB in the charging profile corresponds to α -phase wherein the hydrogen is dissolved in the metal lattice. The region BC corresponds to $\alpha + \beta$ -phase wherein the α -phase and β -phase coexist. At the point B, the saturation of α -phase takes place and at the point D, saturation of β -phase takes place. The region CD corresponds to β -phase solid solution. The region DE corresponds to $\beta + \gamma$ -phase. The region EF corresponds to γ -phase hydride. These phase transformations during electrochemical hydrogenation are analogous to the gas phase hydrogenation obtained by Nakamura et al. [15]. These phase transformation is also seen at C/5 rate but limited up to DE region since the charging was performed up to the point E. If the charging was performed continuously the same pattern would have been obtained

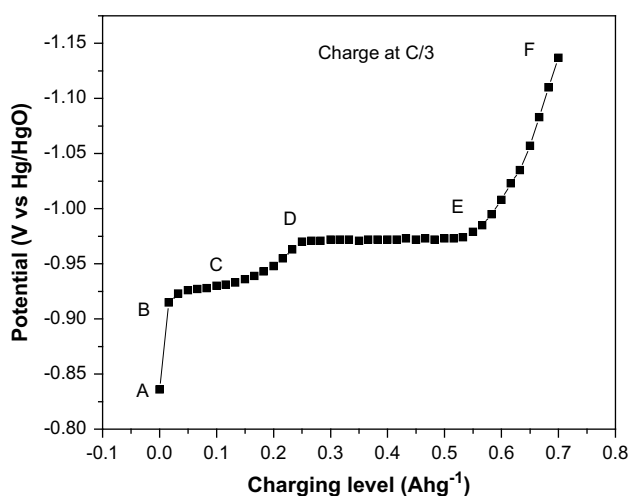


Fig. 2 – Phase transformation of $\text{MmNi}_{3.03}\text{Si}_{0.85}\text{Co}_{0.60}\text{Mn}_{0.31}\text{Al}_{0.08}$ alloy metal hydride electrode during charging (C/3 charge).

indicating the different phase changes. However, these phase differentiations do not exist for other charging rates as seen from the charging profiles. These may be due to the rise in temperature at higher charging current densities.

The specific discharge level of metal hydride electrode after various rate of overcharge is represented in Fig. 3. The galvanostatic discharge experiments were carried out at C/5 rate and the cutoff potential was -0.7 V with respect to Hg/HgO reference electrode. The discharge level is 255, 250, 259, 254, 249 and 239 mAhg^{-1} at C/5, C/3, 1C, 2C, 3C and 4C, respectively. The discharge level remains almost constant and there is not much change once the electrode is overcharged. From this observation, it can be concluded that the metal hydride electrode is capable of accepting the overcharge. However the energy spent for overcharge can be utilized for heat generation and consequently for the hydrogen evolution reaction which is detrimental to the performance of catalytic activity during hydrogen absorption and desorption.

The potential profile of metal hydride electrode charged at various rates i.e. C/5, C/3, 1C, 2C, 3C and 4C as a function of the electric charge level is shown in Fig. 4. During these charging processes, the overall charge input given to the electrode is 3.36 Ah. The charging profiles indicate the sudden upward increase in potential and a sloping region especially in 2C, 3C and 4C charging and then the potential decreases. The hydrogen absorption comes to a halt at the end of the sloping region and thereafter hydrogen evolution takes place as explained earlier. The increase in potential is seen as the current density increases. The two reactions that occur at the electrode during charging are charge transfer at the electrode–electrolyte interface and hydrogen diffusion into the bulk. The charge-transfer reaction at the interface is faster than the hydrogen absorption. A higher charging current density leads to a rapid increase in the hydrogen concentration at the alloy particle surface. The accumulated hydrogen at the surface does not diffuse quickly enough into the alloy causing an increase in the equilibrium pressure and hence in the potential. Hydrogen evolution also takes place which is responsible

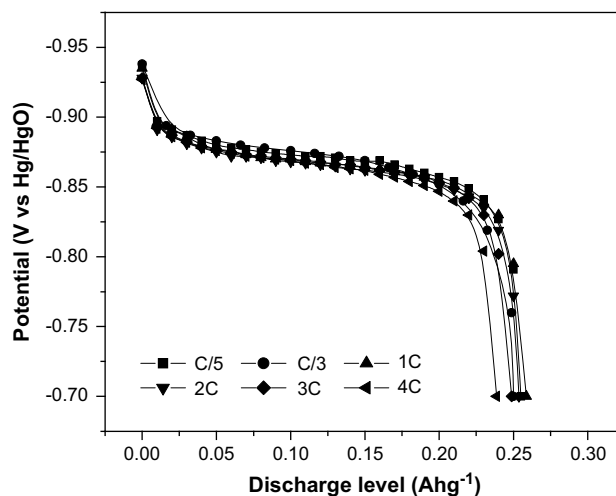


Fig. 3 – Discharge profiles of $\text{MmNi}_{3.03}\text{Si}_{0.85}\text{Co}_{0.60}\text{Mn}_{0.31}\text{Al}_{0.08}$ alloy metal hydride electrode at C/5 rate after overcharge at various rates.

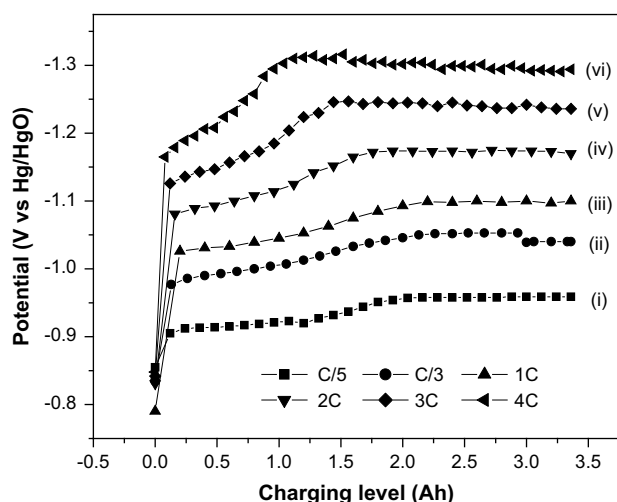


Fig. 4 – Charging profiles of $MmNi_{3.03}Si_{0.85}Co_{0.60}Mn_{0.31}Al_{0.08}$ alloy metal hydride electrode at various current density.

for the decrease in the voltage profile after reaching a saturation of the hydrogen adsorption/absorption.

Fig. 5 shows the discharge level at C/5 rate after the electrode is charged at various high rates. In the entire charging rate the charge input provided is 3.36 Ah. The observed discharge levels are 246, 250, 246, 243, 241 and 240 $mAhg^{-1}$ after C/5, C/3, 1C, 2C, 3C and 4C rate, respectively. The loss of discharge level for 4C rate with respect to the C/5 one is only 2.5%. This indicates that the metal hydride alloy has excellent charge acceptance and the electrode could be charged at higher rate. The rate dependent capacity measurements were also carried out and the discharge profiles relative to the various discharge current densities are depicted in Fig. 6. The discharge level obtained is 250, 240, 205, 164, 118 and 58 mAg^{-1} at C/5, C/3, 1C, 2C, 3C and 4C, respectively. In 4C rate, the cell delivers about 23% of the discharge level obtained at C/5 rate.

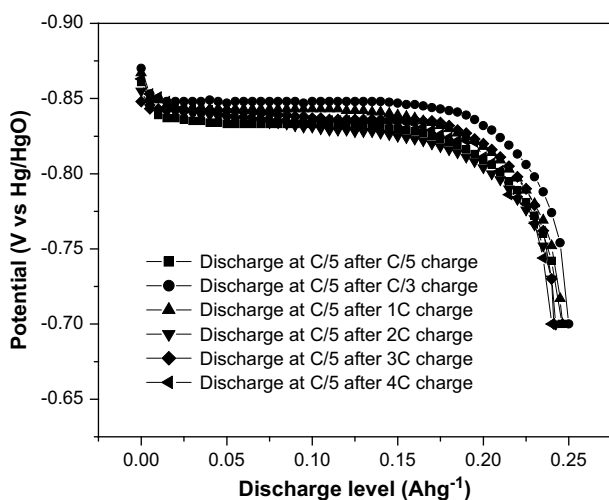


Fig. 5 – Discharge profiles of $MmNi_{3.03}Si_{0.85}Co_{0.60}Mn_{0.31}Al_{0.08}$ alloy metal hydride electrode at C/5 rate after charging at various rates (restricted to 3.36 Ah).

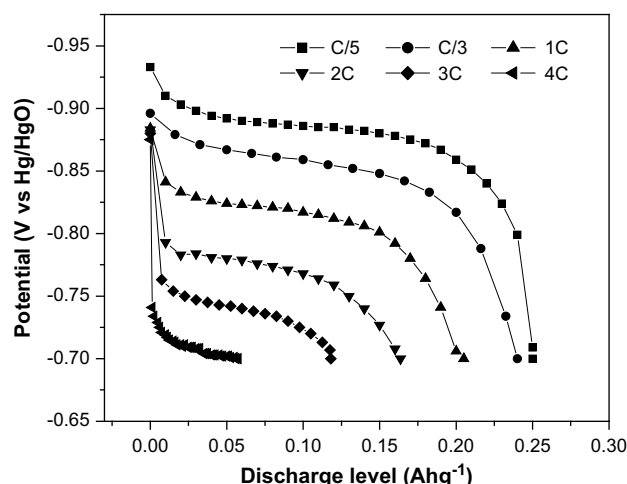


Fig. 6 – Discharge curves of $MmNi_{3.03}Si_{0.85}Co_{0.60}Mn_{0.31}Al_{0.08}$ alloy metal hydride electrode at various rates.

The essential parameter of a battery for application with an electric car is the high capacity i.e. the total amount of charge which can be recovered during galvanostatic discharge. The high-rate dischargeability (HRD) is defined as the ratio of the discharge level, Q_i at the cutoff potential of -0.7 V with respect to the reference electrode at the discharge current density, I_d to the maximum discharge level, Q_{max} [16]

$$HRD = \frac{Q_i}{Q_{max}} \times 100\% \quad (1)$$

The high-rate dischargeability of the metal hydride electrode is represented in Fig. 7 in relation to the discharge level obtained at C/5 rate. The high-rate dischargeability is 96%, 82%, 66%, 47% and 23% at C/3, 1C, 2C, 3C and 4C, respectively. It can be seen that the HRD of metal hydride electrode decreases monotonously as the current density increases. It is generally accepted that the HRD of a metal hydride electrode

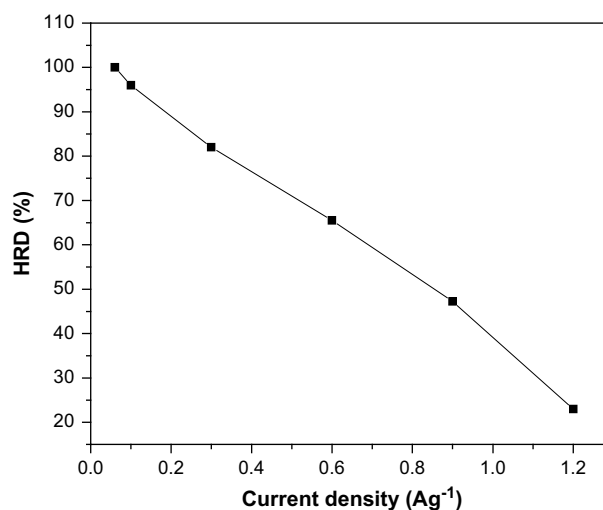


Fig. 7 – High-rate dischargeability of $MmNi_{3.03}Si_{0.85}Co_{0.60}Mn_{0.31}Al_{0.08}$ alloy metal hydride electrode.

Table 1 – Hydrogen diffusion at various discharge rates.

Discharge rate	Current density (mA g ⁻¹)	Diffusion coefficient (×10 ⁻¹⁰ cm ² s ⁻¹)
C/5	60	5.72
C/3	100	2.81
1C	300	1.96
2C	600	1.82
3C	900	1.77
4C	1200	1.75

is mainly determined by the charge-transfer process occurring at the electrode–electrolyte interface and the hydrogen diffusion process in the bulk. During the discharge process, hydrogen diffuses from the bulk to the surface of the alloy powder. Hydrogen diffusion in the metal hydride electrode dominates the high-rate discharge capability. At higher discharge current densities a fast decrease in the hydrogen concentration at the powder surface and the accumulated OH⁻ ions lead to the formation of a passivation layer [17]. This passivation layer restricts the charge-transfer process and hence leads to a decrease in the discharge level at the higher discharge current density.

Apart from the kinetics of the process occurring at the metal hydride electrode/electrolyte interface, the rate of hydrogen diffusion within the bulk of the hydrogen absorbing alloy is also the important factor that controls the performance of the metal hydride electrode. An evaluation of the hydrogen diffusion in a charge discharge reaction is influenced both by micro- and macro-structure of the alloy. The diffusion coefficient of atomic hydrogen in the solid phase has been shown to depend on the strength of the metal–hydrogen interaction and on the hydrogen concentration in the bulk. However, the hydrogen diffusion coefficient (*D*) was calculated with a galvanostatic discharge technique proposed by Zheng et al. [18]:

$$D = \frac{i_d r^2}{15(Q_0 - \tau i_d)} \quad (2)$$

where *i_d* = Discharge current density (A/g), *r* is the average radius of the alloy particle (cm), *Q₀* is the initial specific electric charge (C/g⁻¹), and *τ* is transient time (s), i.e. the time required for the surface concentration of hydrogen to become zero. The calculated diffusion coefficient values at various current densities are listed in Table 1. It can be seen from Table 1 that the diffusion coefficient decreases as the current density increases. The passivation layer formed at the higher current densities on the surface of the alloy powder could prevent the diffusion of hydrogen and hence led to the decrease in diffusion coefficient at higher discharges current density.

4. Conclusions

The success of a battery for electric vehicles depends critically on the high-rate charge/dischargeability characteristics apart from other parameters. Galvanostatic charge–discharge experiments were performed at various rates on the negative electrode prepared from MmNi_{3.03}Si_{0.85}Co_{0.60}Mn_{0.31}Al_{0.08}

metal hydride alloy. It was observed that the electrode has excellent rapid charge acceptance. The charging curves especially at C/3 rate are indicative of phase changes occurring during hydrogen absorption. The high-rate dischargeability of metal hydride electrode decreases monotonously with increase in current density. The diffusion coefficient of hydrogen decreases with increase in discharge current density.

Acknowledgements

The authors thank the Director, CECRI for his encouragement and permission to publish this work. Thanks are also due to Dr. N.G. Renganathan of Electrochemical Power Systems Division, CECRI and Dr. G. Balachandran of the Rare Earth Processing Group, DMRL, Hyderabad for discussions and for preparing the alloy, respectively. Thanks are also due to Ministry of New and Renewable Energy (MNRE), New Delhi for sanctioning a Grant-In-Aid project on ‘Development of Advanced Ni–MH Battery fitted Electric Cycle and Field Studies’ as some of the project facilities were used for the above work.

REFERENCES

- [1] Viera JC, González M, Liaw BY, Ferrero FJ, Álvarez JC, Campo JC, et al. Characterization of 109 Ah Ni–MH batteries charging with hydrogen sensing termination. *J Power Sources* 2007;171:1040–5.
- [2] Zhan F, Jiang LJ, Wu BR, Xia ZH, Wei XY, Qin GR. Characteristics of Ni/MH power batteries and its application to electric vehicles. *J Alloys Compd* 1999;293–295:804–8.
- [3] Liaw BY, Yang XG. Limiting mechanism of rapid charging Ni–MH batteries. *Electrochim Acta* 2001;47:875–84.
- [4] Yang XG, Liaw BY. Fast charging nickel–metal hydride traction batteries. *J Power Sources* 2001;101:158–66.
- [5] Yang HB, Fukunaga H, Ozaki T, Iwakia T, Tanase S, Sakai T. Investigation on substrates of MmNi₅-based alloy electrodes for high power applications. *J Power Sources* 2004;133:286–92.
- [6] Nelson RF. Power requirements for batteries in hybrid electric vehicles. *J Power Sources* 2000;91:2–26.
- [7] Geng M, Han J, Feng F, Northwood DO. Characteristics of the high-rate discharge capability of a nickel/metal hydride battery electrode. *J Electrochem Soc* 1999;146:3591–5.
- [8] Liaw BY, Yang XG. Reliable fast recharge of nickel metal hydride cells. *Solid State Ionics* 2002;152–153:217–25.
- [9] Jordy C, Liska JL, Saft M. In: Proceedings of the 16th electric vehicles symposium Beijing; 1999.
- [10] Nagarajan GS, Van Zee JW. Characterization of the performance of commercial Ni/MH batteries. *J Power Sources* 1998;70:173–80.
- [11] Ananth MV, Raju M, Manimaran K, Balachandran G, Nair LM. Influence of rare earth content on Mm-based AB₅ metal hydride alloys for Ni–MH batteries – an X-ray fluorescence study. *J Power Sources* 2007;167:228–33.
- [12] Raju M, Ananth MV, Vijayaraghavan L. Influence of temperature on the electrochemical characteristics of MmNi_{3.03}Si_{0.85}Co_{0.60}Mn_{0.31}Al_{0.08} hydrogen storage alloys. *J Power Sources* 2008;180:830–5.

- [13] Shi J, Wu F, Chen S, Zhang C. Thermal analysis of rapid charging nickel/metal hydride batteries. *J Power Sources* 2006;157:592–9.
- [14] Ikoma M, Yuasa S, Yuasa K, Kaida S, Matsumoto I, Iwakura C. Charge characteristics of sealed-type nickel/metal-hydride battery. *J Alloys Compd* 1998;267:252–6.
- [15] Nakamura Y, Nomiya T, Akiba E. Phase transformation in $\text{La}(\text{Co}_x\text{Ni}_{5-x})$ -systems ($x = 2, 3, 5$) studied by in situ X-ray diffraction. *J Alloys Compd* 2006;413:54–62.
- [16] Pan H, Ma J, Wang C, Chen S, Wang X, Chen C, et al. Studies on the electrochemical properties of $\text{M}(\text{Ni}_{4.3-x}\text{Co}_x\text{Al}_{0.7})$ hydride alloy electrodes. *J Alloys Compd* 1999;293–295:648–52.
- [17] Geng M, Feng F, Han J, Matchett AJ, Northwood DO. Anodic polarization and galvanostatic investigation of a metal hydride alloy electrode. *Int J Hydrogen Energy* 2001;26:133–7.
- [18] Zheng G, Popov BN, White RE. Determination of transport and electrochemical kinetic parameters of bare and copper-coated $\text{LaNi}_{4.27}\text{Sn}_{0.24}$ electrodes in alkaline solution. *J Electrochem Soc* 1996;143:834–9.